JOURNAL OF MAGNETIC RESONANCE **135,** 185–193 (1998)
ARTICLE NO. MN981543

H(C)CH-COSY and (H)CCH-COSY Experiments for ^{13}C-Labeled Proteins in H_2O Solution

Kalle Gehring* and Irena Ekiel†

**Department of Biochemistry and Montreal Joint Centre for Structural Biology, McIntyre Medical Science Building, McGill University, 3655 Drummond Street, Montreal, Quebec, H3G 1Y6, Canada; and †Pharmaceutical Biotechnology Sector and Montreal Joint Centre for Structural Biology, Biotechnology Research Institute, National Research Council of Canada, Montreal, Quebec, H4P 2R2, Canada*

E-mail: kalle.gehring@bri.nrc.ca

Received March 18, 1998; revised June 22, 1998

We present three experiments which serve to identify carbon and proton sidechain resonances in ^{13}C-labeled proteins. The first is an improvement on the previously published H(C)CH-COSY experiment and comprises the application of gradients for coherence selection and a reduction in the phase cycle. The second experiment is a new (H)CCH-COSY with two carbon dimensions. The (H)CCH-COSY presents several advantages over the H(C)CH-COSY experiment in terms of better sensitivity, improved resolution and easier identification of amino acid spins systems. The third experiment is a 2D proton-edited (H)C(C)H-COSY that allows suppression of methylene resonances. All three HCCH-COSY experiments show good sensitivity and excellent solvent suppression. The 2D version can be acquired in as little as 45 minutes and the 3D versions acquired overnight. The experiments are demonstrated on a ^{13}C-labeled sample of the second PDZ domain from human phosphatase PTP1E in H_2O solution.

Key Words: **heteronuclear NMR; correlation spectroscopy; pulsed field gradients; solvent suppression.**

INTRODUCTION

The utility of carbon–carbon COSY spectra in assigning sidechain resonances of proteins is well established (*1–7*). Using large one-bond H–C and C–C couplings, H(C)CH-COSYs avoid sensitivity problems due to large proton linewidths and small couplings and allow the identification of vicinal proton and carbon pairs. HCCH-COSYs also benefit from resolution of overlapped proton resonances through carbon labeling.

Since its first introduction (*1*), several technical improvements to the H(C)CH-COSY experiment have been described. The first of these was a replacement of the carbonyl composite pulse decoupling in t1 and t2 by selective 180° pulses along with a modification of the 16-step phase cycle (*3*). More recently, constant-time evolution in the t2 evolution period was introduced leading to better sensitivity and pure absorption lineshapes (*2*).

Here, we describe a new experiment, (H)CCH-COSY, with two carbon dimensions and outline several additional modifications to the H(C)CH-COSY for use on samples in H_2O with a much reduced phase cycle. These improvements are made possible by the inclusion of coherence-selective gradient pulses and purge pulses on carbon and proton. The shorter phase cycle permits the acquisition of excellent quality spectra in as little as 7 hours. Alternatively, for less concentrated samples that require longer acquisition times, the carbon spectral window can be expanded to avoid aliasing in t2 which simplifies spectral analysis.

The (H)CCH-COSY is the complement of the better known proton–carbon–proton experiment and correlates two carbon frequencies. (H)CCH labeling has several advantages over the H(C)CH experiment. The first is much better sensitivity due to constant-time labeling in carbon and a reduction in the number of methylene peaks. Equally significantly, the resolution in the carbon dimensions is significantly better than in the proton dimensions. Finally, the interpretation of the (H)CCH spectrum is more straightforward (*8, 9*).

Together, the two COSY experiments provide nearly complete proton–carbon assignments. Sample spectra of an ^{15}N,^{13}C-labeled sample of a PDZ domain from the hPTP1E phosphatase are presented (*10*). Experimental times ranged from overnight for the accumulation of a *pair* of H(C)CH-COSY and (H)CCH-COSY spectra to 45 min for a 2D (H)C(C)H-COSY with spectral editing.

RESULTS AND DISCUSSION

Figure 1 shows the pulse sequences for the HCCH-COSY experiments with either carbon (top panel) or proton (bottom panel) labeling in the first (t1) dimension. As the pathway of magnetization transfer in the experiments has been described previously (*2*), only details related to the improvements suggested here will be described. One significant difference between our H(C)CH-COSY pulse sequence and previous sequences is the labeling of the second rather than the first carbon

1090-7807/98 $25.00

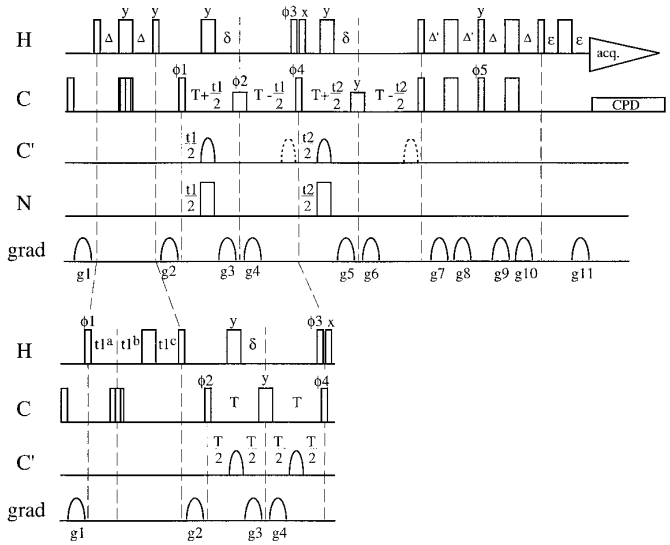

FIG. 1. Pulse sequence of (H)CCH-COSY (top) and H(C)CH-COSY (bottom) experiments. Following the pulses $\phi 3$ and $\phi 4$, both experiments are identical and only the (H)CCH-COSY sequence is shown. Thin and thick pulses correspond to 90° and 180° flip angles, respectively. The first aliphatic carbon 180° pulses are hatched to indicate that they were composite 90°(−y)–180°(x)–90°(−y) pulses. Half-height 180° aliphatic C pulses were attenuated squarewave pulses (9.5 kHz) adjusted to provide a null in the excitation profile at the C′ frequency. Carbonyl pulses were sinebell shaped 180° pulses of 242 μs applied as phase-shifted laminar pulses (*28, 29*). Dashed carbonyl pulses are for Bloch–Siegert shift compensation but can be advantageously omitted in order to lengthen the t1 and t2 labeling periods. Carrier frequencies were 46.5 ppm for $C^{aliphatic}$, 176 ppm for C′, and 4.7 ppm for protons. Delays were $\Delta = 1.7$ ms, $\Delta' = 1.1$ ms, $\delta = 2.8$ ms, $\epsilon = 1$ ms, $T = 3.9$ ms, $\tau = T + t1/2$, $\tau' = T - t1/2$, $t1^a = 3$ μs (initial), $t1^b = 3$ μs (initial), $t1^c = 1.7$ ms (initial). For t1 frequency labeling in the H(C)CH-COSY experiment, $t1^a$ was incremented and $t1^c$ decremented until $t1^c$ approached zero. Then, for the remainder of t1, $t1^b$ was incremented. Gradients were sinebell shaped with a duration of 0.8 ms and were followed by a recovery delay of 0.2 ms. Gradient strengths (Gauss/cm) and axes (x, y, z) were g1 = (0, −33.5, 0), g2 = (0, 33.5, 0), g3 = g4 = (23.5, 0, 0), g5 = (−26.8, 0, 0), g6 = (−26.8, 0, −67), g7 = g8 = (0, 23.5, 0), g9 = g10 = (0, −26.8, 0), g11 = (0, 0, 16.8). Gradients g6 and g11 provide the coherence selection with the sign of g6 changing in alternate FIDs. Phase-cycling of the pulses and receiver was as follows. For the (H)CCH-COSY, $\phi 1 = x, \phi 2 = x, y, -x, -y; \phi 3 = x, x, -x, -x; \phi 4 = x, -x, -x, x; \phi 5 = y$, receiver $= x, -x$. Phase $\phi 1$ was cycled in a States-TPPI manner to provide quadruature detection in t1. Proton pulse $\phi 3$ and the following proton pulse were applied with no interpulse delay so as to administer either a 180° or 0° pulse according phase $\phi 3$. Phase $\phi 5$ was cycled in concert with the sign of gradient g6 to provide phase sensitive detection in t2. For the H(C)CH-COSY, phases were identical except for $\phi 2 = x, -x$. For the 2D version of the (H)CCH-COSY, the (H)CCH-COSY pulse sequence was used with the t2 increment fixed at 3 μs. Gradients g3 and g4 were omitted to prolong the t1 carbon labeling period and a more complete sixteen-step phase cycle was used: $\phi 1 = x, \phi 2 = x, y, -x, -y; \phi 3 = 2(x), 2(-x), 2(x), 2(-x), 2(-x), 2(x), 2(-x), 2(x); \phi 4 = x, -x, -x, x, -x, x, x, -x; \phi 5 = y$ (not cycled), receiver $= x, -x$. In most cases, the phase of the attenuated aliphatic carbon 180° pulses must be manually adjusted due to Bloch–Siegert effects and phase differences between the carbon pulses at different power levels. Pulses for which a phase is not indicated were applied along the x axis.

nucleus. As described below, this improves the H(C)CH-COSY sensitivity at a cost of slightly less balanced resolution before and after the COSY mixing pulse.

In both sequences, a carbon purge pulse is applied at the beginning of the experiment to eliminate unwanted carbon magnetization. For the (H)CCH experiment, this has the distinct advantage of shortening the phase cycle by elimination of phase cycling of the first proton pulse.

Following the ^{13}C purge pulse, magnetization starts on protons and is transferred by an INEPT sequence to the directly attached carbon. Proton labeling in the H(C)CH-COSY is carried out using a semi-constant time or "shared-time" scheme (*11, 12*). Although this complicates the acquisition (the data set is acquired as two experiments on our Bruker DRX500 spectrometer), the semi-constant time scheme improves both the sensitivity of the experiment and lineshape in t1. Because of a limitation in the number of gradient pulses that our spectrometer hardware can implement, we were unable to add gradient pulses around the proton and carbon 180° pulses in the first INEPT sequence. While unnecessary for the (H)CCH experiment, the additional gradient pulses might have improved the water suppression in the H(C)CH-COSY (see below). In both pulse sequences, a ZZ filtering gradient (g2) is employed at the end of the first INEPT sequence.

In the (H)CCH experiment, carbon frequency labeling in t1 is carried out in a constant-time manner as described previously (*2*). The length of the carbon labeling period is limited to ~7.8 ms during which carbon–carbon antiphase magnetization develops. This delay is kept short to optimize magnetization transfer between carbons with more than one carbon coupling partner. Inclusion of gradients in the t1 period further reduces the length of the labeling period to only ~6 ms. Hence, two types of (H)CCH experiments were tested: one with gradients in t1 and one without gradients. The gradient version (shown in Fig. 1) gave slightly better artifact suppression and is preferable in the 3D experiments. The artifacts in the non-gradient version could be suppressed by a longer phase cycle and this version was used in 2D experiments. An additional advantage of the non-gradient version is that the two carbonyl decoupling pulses could be placed midway between the surrounding aliphatic carbon 90° and 180° pulses. This allows use of a "high power" aliphatic 180° pulse since no carbonyl magnetization is present at the time of the aliphatic 180° pulse. In the gradient version, an attenuated aliphatic 180° pulse has to be used to avoid perturbing the evolving carbonyl magnetization (*13*). The alternative of centering the carbonyl decoupling pulses with pulsed field gradients would require either their simultaneous application or unacceptably shorten the t1 evolution times.

During the t1 carbon labeling period [and corresponding period in the H(C)CH-COSY], carbon–carbon antiphase magnetization develops while at the same time refocusing with respect to the attached proton(s). As suggested by Bax and co-workers, spectral editing can be performed by varying the position of the 180° proton pulse preceding the delay δ (*1, 2*). An effective proton–carbon evolution time of 2.2 ms ($\delta = 2.8$ ms) allows all carbons to partially refocus and is optimal for obtaining a spectrum with signals from all carbon types. A

longer evolution time of 4 ms ($\delta = 1.9$ ms) allows selection for methine carbons (see below).

The carbon 90° pulse with phase $\phi 4$ is the mixing pulse that transfers magnetization from the first to second carbon. The addition of a proton purge pulse (phase $\phi 3$) at this point greatly improved artifact suppression for diagonal peaks in the (H)CCH-COSY experiment. This is because not all of carbon magnetization is in-phase with respect to attached protons at the time of the carbon mixing pulse. For diagonal peaks, this magnetization can refocus and leads to a strong phase twist that was particularly apparent in the F1/F3 lineshapes of diagonal methyl peaks. Phase alternation of the proton purge pulse was used to remove carbon magnetization with antiphase proton terms and gave pure absorption lineshapes.

Two different types of proton purging pulses were tested. In early experiments, a single 90° proton pulse was used to convert longitudinal proton magnetization into unobservable double/zero quantum magnetization. Phase alternation of this proton pulse and co-addition of the FIDs very effectively removed the dispersive lineshapes in F1/F3. However, closer examination of the spectra revealed that application of a 90° proton purge pulse introduced a new distortion in the F2 dimension. This appeared to be limited to CH_2 carbons with non-degenerate proton frequencies. As an alternative to a single 90° pulse, a second scheme was tried in which two proton pulses were applied to give alternately a 0° or 180° pulse as shown in Fig. 1. The rationale was that diagonal peaks with an odd number of longitudinal proton terms would still be cancelled by the phase cycle while signals with two proton terms would no longer give rise to transverse proton terms and phase distortions in the F2 dimension. The only disadvantage to the 0°/180° phase cycle was slightly poorer water suppression in the 3D H(C)CH experiment. This could probably be improved by the addition of gradients to stabilize the water signal during t1.

The effect of the proton purge pulse in the (H)CCH-COSY can be explained using product operator formalism. For diagonal peaks, magnetization is present in up to eight different magnetization states for methyl resonances (or six states for methylene or four for methine resonances) at the time of the carbon mixing pulse,

$$\cos(\omega_1 \cdot t1)[C_{1x} + 2C_{1y}I_z + 4C_{1x}I_{1z}I_{2z} + 8C_{1y}I_{1z}I_{2z}I_{3z}] + \sin(\omega_1 \cdot t1)[C_{1y} + 2C_{1x}I_z + 4C_{1y}I_{1z}I_{2z} + 8C_{1x}I_{1z}I_{2z}I_{3z}],$$

where I_{1z}, I_{2z}, and I_{3z} refer to different protons, C_{1x} and C_{1y} refer to the first carbon nucleus. Constant terms related to relaxation or J-couplings have been omitted. For crosspeaks, the expression can be greatly simplified since terms with antiphase proton magnetization need not be retained. Therefore, crosspeaks arise from only the carbon antiphase terms:

$$\sin(\omega_1 \cdot t1)2C_{1x}C_{2z} + \cos(\omega_1 \cdot t1)2C_{1y}C_{2z}.$$

The carbon mixing pulse is applied with a two-step phase cycle (x, $-x$) and selects for magnetization with $\cos(\omega_1 \cdot t1)$ terms. For cross peaks, the mixing pulse yields

$$\cos(\omega_1 \cdot t1)2C_{1z}C_{2y}$$

which evolves into

$$\cos(\omega_1 \cdot t1)\cos(\omega_2 \cdot t2)2C_{2y}I_{4z} + \cos(\omega_1 \cdot t1)\sin(\omega_2 \cdot t2)2C_{2x}I_{4z}$$

prior to the planar echo transfer.

For diagonal terms, phase alternation of the mixing pulse and co-addition eliminates diagonal terms with C_{1y} magnetization and leaves only terms

$$\cos(\omega_1 \cdot t1)[C_{1x} + 4C_{1x}I_{1z}I_{2z}] + \sin(\omega_1 \cdot t1)[2C_{1x}I_{1z} + 8C_{1x}I_{1z}I_{2z}I_{3z}].$$

In order to obtain in-phase diagonal peaks, we need to eliminate the $\sin(\omega_1 \cdot t1)$ term. This can be done by either purging all antiphase proton magnetization with a 90° proton pulse (which generates 2 $C_{1x}I_{1y}$, 4 $C_{1x}I_{1y}I_{2y}$ and 8 $C_{1x}I_{1y}I_{2y}I_{3y}$ magnetization) or co-addition of signals acquired with 0°/180° pulses on protons. In the latter case, only terms with an odd number of proton operators are cancelled. Although both purging pulse schemes worked well in eliminating out-of-phase diagonal terms in F1/F3 dimensions, the 90° proton pulse generates zero quantum $I_1^+I_2^-$ magnetization that is not suppressed by gradients in t2. During the planar echo transfer, this magnetization is converted into observable magnetization by the first proton 90° pulse and phase distortion in F2 results.

Following the carbon mixing pulse ($\phi 4$), the pulse sequence is essentially reversed leading to transfer back to protons. As coherence selection with pulsed field gradients is employed, gradients g5 and g6 cannot be omitted and the carbon t2 labeling period mirrors the t1 labeling period in the t1-gradient version. During the t2 period, carbon–carbon magnetization must refocus while at the same time defocusing with respect to a proton on the second carbon. Application of the off-resonance carbonyl decoupling pulses in the carbon labeling periods leads to a Bloch–Siegert shift of the aliphatic resonances. As indicated in Fig. 1, this shift can be removed by application of compensatory carbonyl pulses at the end of the carbon labeling periods (*13*).

Following t2, a planar echo is used to transfer magnetization from carbon to its attached proton (*14, 15*). This allows gradients to be used for coherence selection and provides exceptional water suppression (*16–19*). Gradients g6 and g11 provide the coherence selection. Gradient g6 also serves to refocus magnetization from g5 following the aliphatic C 180° pulse. Incorporation of gradients g7–g10 improves the water suppression without phase cycling of pulses in the planar echo sequence. The suppression of signals not attached to carbon was

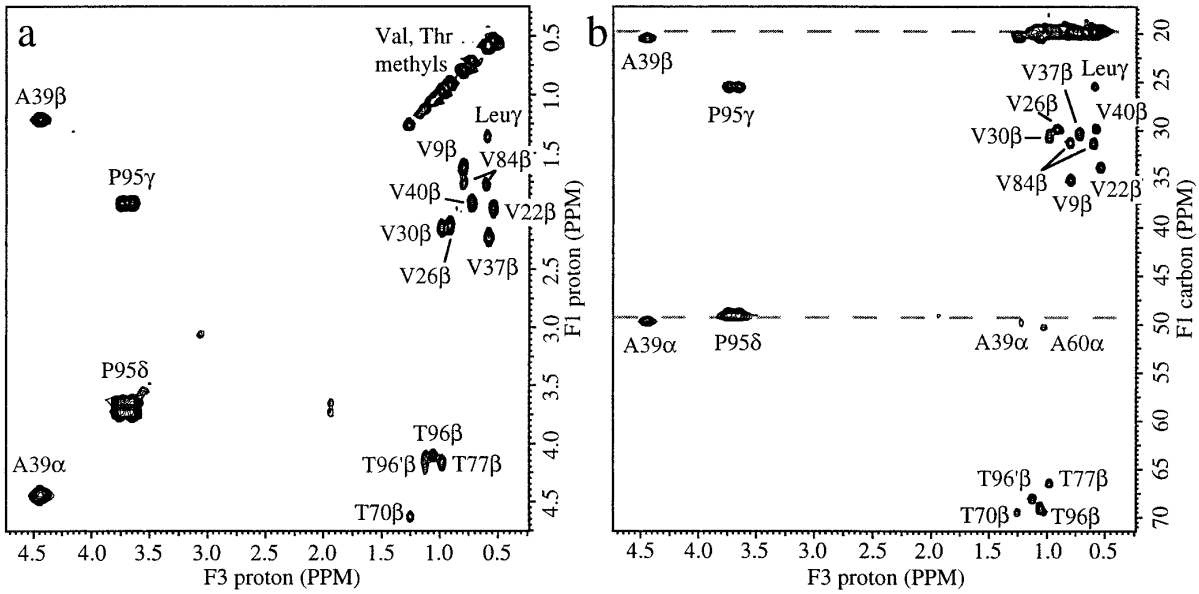

FIG. 2. F1/F3 slices of (H)CCH-COSY and H(C)CH-COSY spectra of the hPTP1E PDZ-2 domain complexed to a 15 amino acid peptide. The carbon F2 dimension was extensively folded to reduce the acquisition time and data size. The planes shown correspond to F2 equal to 49.4 or 19.8 ppm. In the (H)CCH spectrum (panel a), this gives rise to two diagonals as indicated by the dashed lines. Diagonal peaks (F1 = F2) are present for the C^{α} of Ala39, C^{δ} of Pro95, and methyl groups of valine, leucine, and threonine as indicated. The C^{β}/C^{α} cross peaks of Ala39 and Ala60 are more intense on the previous F2 plane. In the H(C)CH-COSY spectrum (panel b) the proton–proton diagonal (F1 = F3) is visible along with cross peaks for the H^{β}'s of Ala39, $H^{\gamma 1}$, and $H^{\gamma 2}$ of Pro95, and the H^{β}'s and H^{γ} of the valine, leucine, and threonines indicated. Peaks are labeled according to their chemical shift in F1. A weak in-phase signal for Pro95 is seen at F3 = 1.9 ppm. This appears to be a weak COSY transfer artifact that occurs during the planar echo transfer between F2 and F3 dimensions. The (H)CCH-COSY experiment was acquired with 66 (complex) increments in t1 and 22 increments in t2 with sweep widths of 89 ppm and 29.6 ppm, respectively. Total acquisition time was 7.3 h. The H(C)CH-COSY was acquired with 128 complex increments in t1 and a proton sweep width of 8.8 ppm in both F1 and F3 centered at 4.7 ppm. The F2 and F3 dimension were identical in both experiments. Total acquisition time for the H(C)CH-COSY experiment was 13.5 h. In both spectra, the carbon dimension was doubled by Burg linear prediction before apodization by a cosine squared function and zero-filling. Final data sizes were $256 \times 64 \times 300$ real data points in both experiments.

on the order of 10^5 and completely dispels the need to transfer the sample into D_2O.

A second advantage of the planar echo is the transfer of both transverse components from carbon to protons. This allows frequency labeling of carbon to be carried out with no loss of sensitivity in a "sensitivity-enhanced" manner (*14–17*). This is to say that once the planar echo gradient selection has been chosen for solvent suppression, carbon labeling in t2 comes along for free. As is well known, transfer efficiencies depend on the carbon multiplicity and delay Δ' used (*17*). Although from a resolution standpoint, it would be preferable to label the carbon with the indirectly detected (and lower resolution) proton dimension as in the 3D HC(C)H-COSY experiment, this would entail either a 1.4-fold loss in sensitivity or use of an alternative technique for water suppression.

Setup of the experiments on our spectrometer was facilitated by a triple axis gradient probe. Gradient selection was done on the *Z* axis (which has the greatest dephasing power) while purging gradients were applied along the *X* and *Y* axes. The use of three independent axes prevents the formation of gradient-recalled echos and likely improves the final solvent suppression. Although not tried, artifact suppression might be further improved by magic angle gradients (*20*). Similarly, water suppression in the H(C)CH experiment might be improved by using heteronuclear cross polarization in place of the first INEPT step (*21*).

Figures 2 through 5 show representative spectra obtained using the (H)CCH- and H(C)CH-COSY experiments on the 96 amino acid PDZ-2 domain (*10*). Figure 2 shows a pair of (H)CCH- and H(C)CH-COSY experiments acquired together in just under 21 hours. The second dimension (carbon) in both experiments is folded to provide a manageable 3D data set with 64 F1/F3 planes. In Fig. 2, planes at $F2 = 49.4 + N \times 29.6$ ppm (with $N = \cdots -1, 0, 1 \cdots$) are shown. In the folded (H)CCH spectrum, this corresponds to two diagonals (where F1 = F2) at 49.4 and 19.8 ppm. As noted previously (*1*) use chemical shift of the directly attached proton allows unambiguous assignment of the F2 carbon frequency provided the carbon spectral width is at least ~30 ppm.

Direct comparison of F1/F3 planes in the (H)CCH and H(C)CH spectra allows both the proton and carbon frequencies of crosspeaks to be determined. In Fig. 2, there are approximately 15 diagonal peaks in each plane. From the (H)CCH spectrum, the carbon chemical shifts of all the crosspeaks can be measured and, in the H(C)CH spectrum, the proton chemical shifts are present. Together, the exper-

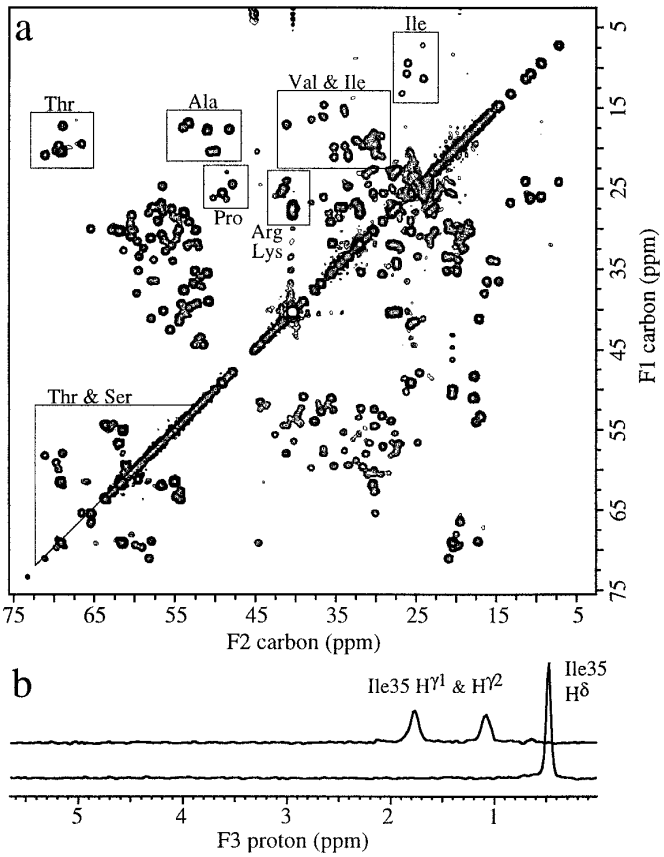

FIG. 3. F1/F2 projection of (H)CCH-COSY spectrum of unliganded hPTP1E PDZ-2. The carbon F2 dimension was not folded and the skyline projection along the proton F3 axis calculated. Although both F1 and F2 are indirect dimensions, they provide excellent resolution and dispersion. (a) Aliphatic region of the F1/F2 carbon-carbon projection. Regions of the spectrum specific for one or two amino acids are boxed. From top to bottom, these are the Ile C^{δ}-C^{γ} cross peaks, valine and isoleucine C^{γ} (methyl) -C^{β} cross peaks, threonine C^{γ}-C^{β} cross peaks, alanine C^{β}-C^{α} cross peaks, proline C^{γ}-C^{δ} cross peaks, and threonine and serine C^{α}-C^{β} cross peaks. (b) One dimensional F3 columns taken through the most upfield Ile C^{δ}-C^{γ} cross peak on both sides of the diagonal. The upper trace shows the two H^{γ} resonances (read at F2 = 24 ppm) and the lower trace shows the H^{δ} methyl resonance at F2 = 7 ppm. The peak-to-peak signal-to-noise ratios for the H^{γ} resonances are nearly 15 to 1. These are the *weakest* isoleucine C^{δ}-H^{γ} crosspeaks. The unaliased (H)CCH-COSY was acquired in 21 h with 128 complex increments in both F1 and F2 and carbon sweep widths of 90 ppm. Both indirect dimensions were doubled by reflected single value decomposition linear prediction and apodized by a cosine squared function before Fourier transformation. The resulting 3D matrix was 256 × 256 × 336 real data points. Following skyline projection, the 2D matrix was inverse transformed and zero-filled in both dimensions before plotting.

iments allow complete identification of the side chains for most amino acids. Leucine presents a special difficulty in that its H^{γ}/C^{γ} and methyl resonances are nearly degenerate in both proton and carbon chemical shifts. Similarly, the carbon resonances of the long side chains of lysine and arginine showed little dispersion.

Comparison of the two spectra also shows that the (H)CCH spectrum has better resolution in F1 than its H(C)CH counterpart. Although acquired with half as many t1 increments (and in half the time), the constant-time carbon dimension(s) in the (H)CCH-COSY can be doubled by linear prediction and apodized to yield a uniform Gaussian-like lineshape. Carbon linewidths are fixed by the t1 or t2 evolution times and give full widths at half height of 85 or 65 Hz depending on whether gradients are used or not. Assuming an 8125-Hz (65 ppm) spectral width, this represents a resolving power of 96 or 125 (equal to the spectral width divided by the linewidth.) In comparison, PDZ methyl, H^{α} and certain methylene proton linewidths are roughly 29, 49, and 65 Hz with complex lineshapes. For a proton spectral width of 3000 Hz (6 ppm), this represents a resolving power of only 103, 61 or 46, respectively. Furthermore, while proton linewidths will increase in larger proteins, the constant-time carbon linewidths are independent of spectrometer field and T_2. (Signal intensities, however, are adversely affected by shorter T_2's.)

Folding of the F2 dimension both shortens the acquisition time and makes the data set smaller. On the other hand, the interpretation of (H)CCH spectrum is facilitated by acquiring without aliasing in F2. The short 4-step phase cycle makes it possible to perform the experiment overnight as shown in Fig. 3. The carbon–carbon F1/F2 planes of the unfolded (H)CCH show excellent resolution and, in fact, are better resolved than the F1/F3 or F2/F3 planes. Figure 3 shows the F1/F2 skyline projection of an unaliased (H)CCH-COSY experiment of PDZ-2. Even without using the F3 dimension, roughly 70% to 80% of the carbon–carbon correlations are resolved.

Along with high resolution, the carbon dimensions afford a simplified interpretation of the spectra due to the location of peaks with F1 = F2 on the diagonal and the clear separation of different carbon types (*7*). As shown in Figs. 3 and 4, the spin systems of alanine, threonine, serine, valine, isoleucine, and the C^{γ}-C^{δ} of prolines are easily identified. In many cases, the number of each amino acid type can be counted in the 2D projection. Problems of spectral overlap in F1/F2 can be resolved by using the F3 (proton) dimension either as 1D columns (Fig. 3b) or as F1/F2 planes.

Enlargements of parts of the (H)CCH F1/F2 projection are shown in Fig. 4. Nearly complete separation of all the C^{α}-C^{β} crosspeaks is achieved in the 2D representation. With the exception of alanines, serines, and threonines, all the C^{α}-C^{β} crosspeaks fall within a 15 × 20 ppm region centered at roughly 52 ppm (C^{α}) and 35 ppm (C^{β}). Inside this region, the C^{α}-C^{β} crosspeaks are not randomly scattered but are grouped into overlapping zones of different residue specificities (*11*). All six leucines are found at upfield C^{α} and downfield C^{β} chemical shifts. Similarly, glutamine, glutamate, and the basic amino acids predominate at high C^{β} chemical shifts. Valines, prolines, and isoleucines predominate at high C^{α} chemical shifts and show a negative correlation between C^{α} and C^{β} chemical shifts. As hPTP1E PDZ-2 contains both regions of α-helix and β-sheet structure (*10*), part of this correlation (seen

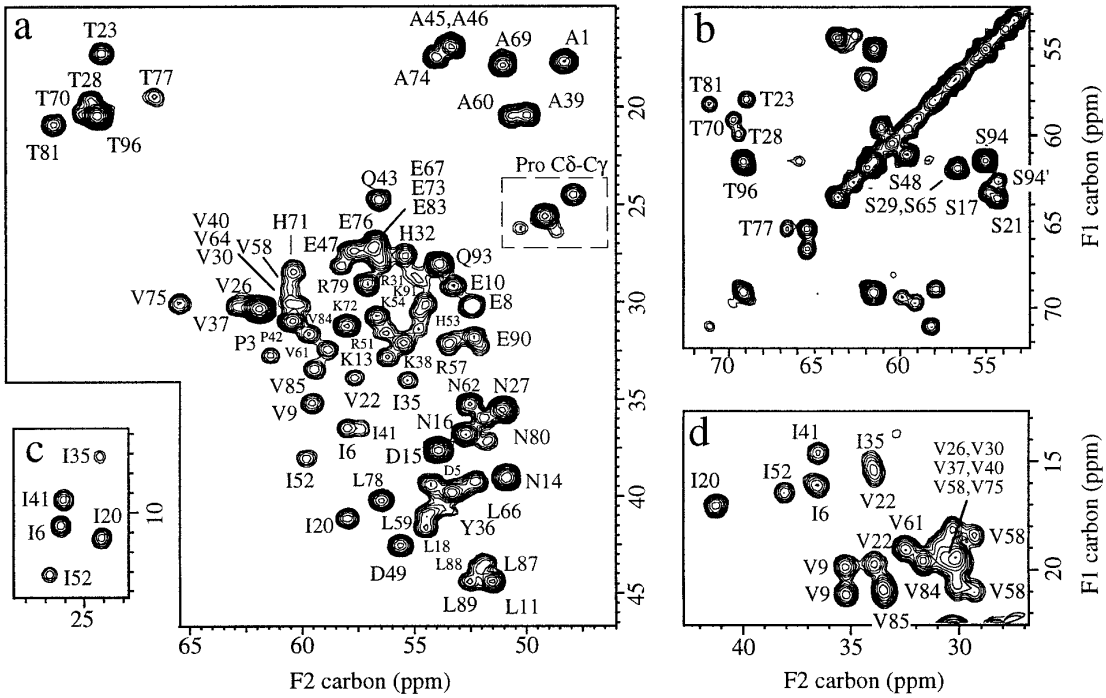

FIG. 4. Enlargement of selected regions of the F1/F2 projection of the (H)CCH-COSY spectrum of unliganded PDZ-2. The regions comprise the majority of C^{α}-C^{β} cross peaks (panel a), threonine and serine C^{α}-C^{β} cross peaks (panel b), isoleucine C^{γ}-C^{δ} cross peaks (panel c), and valine and isoleucine C^{β}-C^{γ} (methyl) cross peaks (panel d). For several amino acids, a second set of weak resonances was observed. We believe that these are related to partial *cis-trans* isomeration of Ser94-Pro95 at the C-terminus.

in several amino acid types) is due to the correlation of chemical shifts with protein secondary structure (*22, 23*).

Proton frequencies can be measured in the unaliased 3D (H)CCH data set by reading columns at a fixed F1/F2. Although the F1/F2 projection appears symmetric, the proton frequencies in F3 differ on the two sides of the diagonal. The F3 proton dimension corresponds to the directly attached proton to the carbon in F2. Two F3 traces for the Ile35 C^{γ}-C^{δ} cross peaks are shown in panel b of Fig. 3. The cross peak above the diagonal gives the two H^{γ} resonances while that below the diagonal gives the methyl H^{δ} chemical shift. Intensity differences between symmetric cross peaks in the F1/F2 projection are due to different peak intensities along the F3 axis. In Fig. 3b, the single methyl resonance has nearly 4 times the peak intensity of the two H^{γ} resonances which leads to a stronger signal in the skyline projection. In a summed (or averaged) projection along F3, cross-peak pairs in the F1/F2 plane are more symmetric in intensity.

The F3 traces also show the excellent sensitivity and solvent suppression in the (H)CCH-COSY. The C^{γ}-C^{δ} cross peak of Ile35 is one of the weaker signals in the spectrum and has a signal-to-noise (*S*/*N*) ratio of roughly 15. Generally, we have found artifact suppression to be a greater problem than sensitivity. This is particularly true for the (H)CCH experiment which is both more sensitive and more difficult to implement. In the H(C)CH-COSY, the difference in nucleus detected before and after the COSY mixing pulse tends to reduce the number of artifacts. In particular, the proton purge pulse (phase $\phi 3$ in Fig. 1) is indispensable in the (H)CCH-COSY but can be omitted from the H(C)CH-COSY (*2*). From a practical standpoint, both experiments should provide acceptable *S*/*N* ratios overnight for samples at <1 m*M*.

At higher fields, cross peaks in the F1/F2 projection of the (H)CCH-COSY will show significantly improved resolution. Although more carbon t1 and t2 increments will be required, the increase in experimental time can be offset somewhat by adjustment of the carbon and proton spectral widths which were not optimized in the present experiments. Even without reducing the spectral widths, the F2 aliased (H)CCH-COSY can be performed in only 18 h at 800 MHz. One caveat is that at higher fields the relative peak intensities may change. While all the peaks have the same lineshape in Figs. 3 and 4, differences in apparent linewidth in the 2D projection are due to differences in transfer efficiency (due to differences in T_2). This reduces the useful resolution as weak peaks are obscured by stronger neighbors. At higher fields, differences between peak intensities will increase as T_2 effects (principally due to carbon CSA) become larger.

At 3.5 m*M*, experiments on the PDZ-2 domain were limited by the length of the phase cycle and number of t1 and t2 increments rather than sensitivity. It was of interest, therefore, to investigate two dimensional versions of the COSY experiments. Previous workers (*2*) had suggested that spectral editing could be performed based on the number of attached protons

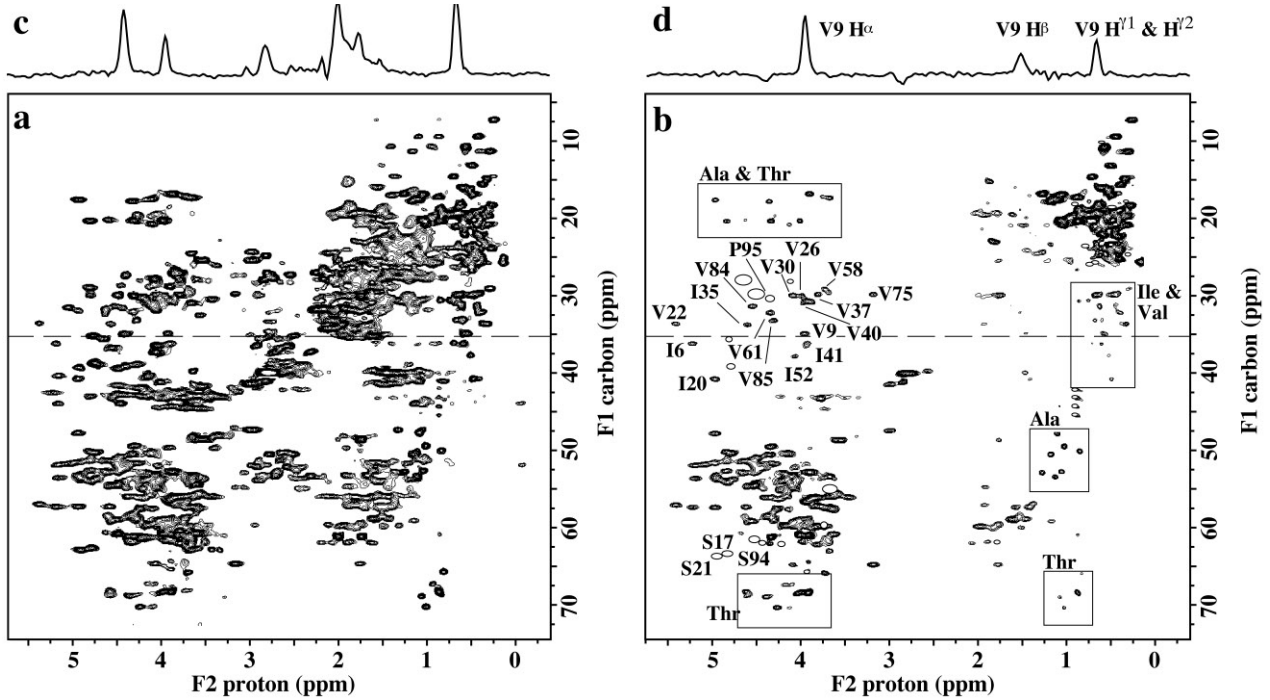

FIG. 5. Two dimensional (H)C(C)H-COSY spectra of unliganded PDZ-2. (a) Aliphatic region of the spectrum acquired with effective proton refocussing delay of 2.2 ms (δ = 2.8 ms in Fig. 1) showing all carbon–carbon correlations. (b) Spectrum acquired with an proton delay of 4.0 ms (δ = 1.9 ms) to select cross peaks between methine carbons. C^{α}-C^{β} cross peaks for the 11 valine and 5 isoleucine residues are indicated along with boxes specific for the indicated amino acids. Methyl resonances were poorly suppressed and numerous CH-CH_3 cross peaks are visible for alanines, threonines, valines and isoleucines. Residues Ser17, Ser21, Ser94 and Pro95 all showed strong negative C^{α}-C^{β} crosspeaks. (c) and (d) Rows from the unedited and edited (H)C(C)H-COSY spectra, taken at the F1 frequency of Val9 C^{β}. Negative peaks in (c) are shown as open ovals. The completely suppressed water signal is at 4.7 ppm. Each experiment was acquired in 45 min using a 16-step phase cycle, 88 complex t1 increments, and 90 ppm carbon sweep width. The carbon dimension was doubled by reflected single value decomposition linear prediction and apodized by a cosine function before zero-filling and Fourier transformation.

and this was applied to a 2D (H)C(C)H experiment (*4*, *24*). The pulse sequence is essentially the same as the 3D (H)CCH-COSY with the substitution of a longer phase cycle in the place of gradients in the t1 frequency labeling period. This increased the resolution in t1 while still keeping the acquisition time relatively short.

Figure 5a shows the relevant portion of the (H)C(C)H spectrum of PDZ-2. A large number of diagonal and cross-peak resonances are present which makes interpretation more difficult than in the F1/F2 projection of the 3D (H)CCH-COSY where peaks arising from magnetization not transferred in the carbon mixing pulse fall on the diagonal (Fig. 3). The superior resolution afforded by the carbon dimension is also clearly apparent. For small proteins, the 2D (H)C(C)H spectrum might provide sufficient resolution to be used in place of the 3D versions. Nonetheless, there is no sensitivity advantage in the 2D experiment (because of the presence of the planar echo) and for an experiment run overnight it is probably worth using the 3D experiment. Projection of the resulting 3D data set along the F2 axis provides the same spectrum as the 2D (H)C(C)H experiment with only slightly poorer resolution in F1.

For concentrated proteins, the 2D (H)C(C)H-COSY has the advantage that it can be run in less than one hour of spectrometer time. This allows the application of spectral editing using different delays for proton refocusing. Figure 5b shows one example of this with identical delays in t1 and t2 to select for methine carbons. The suppression of methyl resonances was only partial but methylene carbons with two attached protons were well suppressed (Fig. 5d). As in DEPT spectra, spectra acquired with different delays can be added and subtracted to select carbons with different numbers of attached protons. The delays in t1 and t2 should be varied separately to select the various CH_1-CH_1, CH_2-CH_2, CH_1-CH_2, CH_1-CH_3, CH_2-CH_3 pairs present. In Fig. 5b, the $C^{\alpha}H_1$-$C^{\beta}H_1$ cross peaks of valine, threonine, and isoleucine are enhanced and easily assigned. Suppression of methylene carbons simplifies considerably the spectrum and allows quick identification of the seven $C^{\alpha}H_1$-$C^{\beta}H_3$ cross peaks of alanines (boxed in Fig. 5b) along with the H^{γ} methyl resonances of valines and isoleucines. Further increasing the effective refocusing time to 6 ms inverted the sign of methylene resonances (data not shown).

CONCLUSIONS

The outlook for studying larger proteins using HCCH-COSY experiments is good. The delays during which carbon

magnetization is in the transverse plane are relatively short (twice 8 ms in the COSY transfer period plus 3 ms in the planar echo transfer) and are comparable to delays in CB-CA(CO)NH or HNCACB experiments (*13, 25*). For the 96 residue PDZ-2 domain, the dispersion of signals in the (H)CCH-COSY F1/F2 projection allowed nearly complete assignment of aliphatic sidechain resonances without using F3. At higher fields and by examining individual F1/F2 planes, it should be possible to assign resonances in proteins with two to three times as many residues. As assignments are made in H_2O solution, using protonated carbons, no isotope or solvent effects need be considered. This should be an advantage when comparing HCCH-COSY spectra with carbon-edited NOESY spectra.

EXPERIMENTAL

NMR spectroscopy. NMR spectra were acquired on a DRX500 spectrometer (Bruker Spectrospin, Milton, Canada) equipped with three RF channels, a three-axis gradient amplifier, and a triple-resonance HCN, three axis pulsed-field-gradient probe.

Sample preparation. (H)CCH- and H(C)CH-COSY experiments were carried out on a 96 amino acid protein, termed PDZ-2, derived from the second PDZ domain in human PTP1E phosphatase (*26*). PDZ-2 was uniformly labeled with ^{13}C and ^{15}N and backbone resonance assignments carried out using standard triple resonance experiments (*10*). Samples were approximately 3.5 m*M* in 90%/10% H_2O/D_2O, pH 6.9, 293 K.

Data processing. All data processing was performed using the Gifa v4 NMR package (*27*).

ACKNOWLEDGMENTS

This work was supported in part by a Medical Research Council of Canada operating grant and salary support to K.G. NRC Publication 41442.

Note added in proof. A carbon-carbon COSY scheme with improved sensitivity for aromatic carbons is reported by K. Pervushin, R. Riek, G. Wider, and K. Wüthrich in "Transverse Relaxation-Optimized Spectroscopy (TROSY) for NMR Studies of Aromatic Spin Systems in ^{13}C-Labeled Proteins," *J. Am. Chem. Soc.* **120,** 6394–6400 (1998).

REFERENCES

1. L. E. Kay, M. Ikura, and A. Bax, Proton-proton correlation via carbon-carbon couplings: A three-dimensional NMR approach for the assignment of aliphatic resonances in proteins labeled with carbon-13, *J. Am. Chem. Soc.* **112,** 888–889 (1990).
2. M. Ikura, L. E. Kay, and A. Bax, Improved three-dimensional ^1H-^{13}C-^1H correlation spectroscopy of a ^{13}C- labeled protein using constant-time evolution, *J. Biomol. NMR* **1,** 299–304 (1991).
3. A. Bax, G. M. Clore, P. C. Driscoll, A. M. Gronenborn, M. Ikura, and L. E. Kay, Practical aspects of proton-carbon-carbon-proton three-dimensional correlation spectroscopy of ^{13}C-labeled proteins, *J. Magn. Reson.* **87,** 620–627 (1990).
4. L. Yu, R. Goldman, P. Sullivan, G. F. Walker, and S. W. Fesik, Heteronuclear NMR studies of ^{13}C-labeled yeast cell wall beta-glucan oligosaccharides, *J. Biomol. NMR* **3,** 429–441 (1993).
5. G. M. Clore, A. Bax, P. C. Driscoll, P. T. Wingfield, and A. M. Gronenborn, Assignment of the side-chain ^1H and ^{13}C resonances of interleukin-1 beta using double- and triple-resonance heteronuclear three-dimensional NMR spectroscopy, *Biochem.* **29,** 8172–8184 (1990).
6. M. Ikura, S. Spera, G. Barbato, L. E. Kay, M. Krinks, and A. Bax, Secondary structure and side-chain ^1H and ^{13}C resonance assignments of calmodulin in solution by heteronuclear multidimensional NMR spectroscopy, *Biochem.* **30,** 9216–9228 (1991).
7. B. H. Oh, W. M. Westler, P. Darba, and J. L. Markley, Protein carbon-13 spin systems by a single two-dimensional nuclear magnetic resonance experiment, *Science* **240,** 908–911(1988).
8. E. T. Olejniczak, R. X. Xu, and S. W. Fesik, A 4D HCCH-TOCSY experiment for assigning the side chain ^1H and ^{13}C resonances of proteins, *J. Biomol. NMR* **2,** 655–659 (1992).
9. S. W. Fesik, H. L. Eaton, E. T. Olejniczak, E. R. P. Zuiderweg, L. P. McIntosh, and F. W. Dahlquist, 2D and 3D NMR spectroscopy employing ^{13}C-^{13}C magnetization transfer by isotropic mixing. Spin system identification in large proteins, *J. Am. Chem. Soc.* **112,** 886–888 (1990).
10. I. Ekiel, D. Banville, S. H. Shen, J. J. Slon-Usakiewicz, A. Koshy, and K. Gehring, Main-chain signal assignment of the PDZ2 domain from human phosphatase hPTP1E and its complex with a C-terminal peptide from the Fas receptor, *J. Biomol. NMR*, in press.
11. S. Grzesiek and A. Bax, Amino acid type determination in the sequential assignment procedure of uniformly $^{13}C/^{15}N$-enriched proteins, *J. Biomol. NMR* **3,** 185–204 (1993).
12. T. M. Logan, E. T. Olejniczak, R. X. Xu, and S. W. Fesik, A general method for assigning NMR spectra of denatured proteins using 3D HC(CO)NH-TOCSY triple resonance experiments, *J. Biomol. NMR* **3,** 225–231 (1993).
13. S. Grzesiek and A. Bax, Correlating backbone amide and side chain resonance in larger proteins by multiple relayed triple resonance NMR, *J. Am. Chem. Soc.* **114,** 6291–6293 (1992).
14. A. G. Palmer, J. Cavanagh, P. E. Wright, and M. Rance, Sensitivity improvement in proton-detected two-dimensional heteronuclear correlation NMR spectroscopy, *J. Magn. Reson.* **93,** 151–170 (1991).
15. J. Cavanagh, A. G. Palmer, P. E. Wright, and M. Rance, Sensitivity improvement in proton-detected two-dimensional heteronuclear relay spectroscopy, *J. Magn. Reson.* **91,** 429–436 (1991).
16. J. Schleucher, M. Schwendinger, M. Sattler, P. Schmidt, O. Schedletzky, S. J. Glaser, O. W. Sørensen, and C. Griesinger, A general enhancement scheme in heteronuclear multidimensional NMR employing pulsed field gradients, *J. Biomol. NMR* **4,** 301–306 (1994).
17. M. Sattler, M. G. Schwendinger, J. Schleucher, and C. Griesinger, Novel strategies for sensitivity enhancement in heteronuclear multidimensional NMR experiments employing pulsed field gradients, *J. Biomol. NMR* **5,** 11–22 (1995).
18. L. E. Kay, P. Keifer, and T. Saarinen, Pure absorption gradient enhanced heteronuclear single quantum correlation spectroscopy with improved sensitivity, *J. Am. Chem. Soc.* **114,** 10,663–10,665 (1992).
19. L. E. Kay, Field gradient techniques in NMR spectroscopy, *Curr. Opin. Struct. Bio.* **5,** 674–681 (1995).

20. P. C. M. Van Zijl, M. O. Johnson, S. Mori, and R. E. Hurd, Magic-angle-gradient double-quantum-filtered COSY, *J. Magn. Reson. A* **113,** 265–270 (1995).

21. H. Wang, and E. R. Zuiderweg, HCCH-TOCSY spectroscopy of ^{13}C-labeled proteins in H_2O using heteronuclear cross-polarization and pulsed-field gradients, *J. Biomol. NMR* **5,** 207–211 (1995).

22. D. S. Wishart, B. D. Sykes, and F. M. Richards, Simple techniques for the quantification of protein secondary structure by ^{1}H NMR spectroscopy, *FEBS Lett.* **293,** 72–80 (1991).

23. S. Spera and A. Bax, Empirical correlation between protein backbone conformation and C^α and C^β ^{13}C nuclear magnetic resonance chemical shifts, *J. Am. Chem. Soc.* **113,** 5490–5492 (1991).

24. T. Szyperski, C. Fernández, and K. Wüthrich, Two-dimensional *ct*-HC(C)H-COSY for resonance assignments of smaller ^{13}C-labeled biomolecules, *J. Magn. Reson.* **128,** 228–232 (1997).

25. M. Wittekind and L. Mueller, HNCACB, a high-sensitivity 3D NMR experiment to correlate amide-proton and nitrogen resonances with the alpha- and beta-carbon resonances in proteins, *J. Magn. Reson. B* **101,** 201–205 (1993).

26. D. Banville, S. Ahmad, R. Stocco, and S.-H. Shen, A novel protein-tyrosine phosphatase with homology to both the cytoskeletal proteins of the band 4.1 family and junction-associated guanylate kinases, *J. Biol. Chem.* **269,** 22,320–22,327 (1994).

27. J.-L. Pons, T. E. Malliavin, and M. A. Delsuc, Gifa V. 4: A complete package for NMR data set processing, *J. Biomol. NMR* **8,** 445–452 (1996).

28. S. L. Patt, Single- and multiple-frequency-shifted laminar pulses, *J. Magn. Reson.* **96,** 94–104 (1992).

29. J. Boyd and N. Soffe, Selective excitation by pulse shaping combined with phase modulation, *J. Magn. Reson.* **85,** 406–413 (1989).